

## Mathematical Modeling of Extraction of Neodymium using Pseudo-emulsion based Hollow Fiber Strip Dispersion (PEHFSD)

Prateek L. Mishra<sup>a</sup>, Biswajit Swain<sup>b</sup>, Anil Kumar Pabby<sup>a\*</sup>, M. L. Singh<sup>c\*\*</sup>,  
S. Gulati<sup>a</sup> & S. Ramasubramaniam<sup>a</sup>

<sup>a</sup>TRP, Nuclear Recycle Board, Tarapur, Maharashtra, 401502

<sup>b</sup>NRPC, Nuclear Recycle Board, Tarapur, Maharashtra, 401502

<sup>c</sup>Nuclear Recycle Board, Mumbai, Maharashtra, 400085

Submitted: 28/7/2021. Revised edition: 18/9/2021. Accepted: 19/9/2021. Available online: 15/11/2021

### ABSTRACT

Pseudo-emulsion based hollow fiber strip dispersion (PEHFSD) is a promising alternative technique due to its stability, simplicity and cost of operation. This is an efficient process due to its high surface area for extraction as well as stripping, and low energy consumption for creating the pseudo-emulsion and for the separation of phases. This technique takes the combine advantages of emulsion liquid membrane and overcomes the sufferings of membrane stability in the supported liquid membrane systems. Present work includes extraction of neodymium (III) ( $N_d$ ) by using TODGA and  $HNO_3$  as the extractant cum strippant in PEHFSD technique. A model is developed to study the transport of  $N_d$  under different hydrodynamic and chemical conditions that includes organic ratio (A/O) in dispersion, effect of speed of impeller on drop size formation, effect of feed acidity, effect of carrier concentration, effect of feed flow rate. A code is written to solve the model equations numerically to predict the concentration of the feed reservoir with time. Experiments are conducted to obtain the best optimum extraction conditions. Results obtained from the numerical simulations are validated with the experimental data and found a good agreement between them.

*Keywords:* Dispersion liquid membrane, Hollow fiber contactor, Modelling, Neodymium ( $N_d$ ), Numerical simulation

### 1.0 INTRODUCTION

Separation of nuclear materials generally is conceded by conventional processes such as solvent extraction and ion exchange. These processes have their own limitations. Usually, the main challenge in designing and operating these devices is to maximize the mass transfer rate by producing as much as interfacial area. For packed columns, selection of packing material and uniform distribution of fluids before they enter the packed bed are big challenges. Alternatively, for devices with moving internals need to

minimize the bubble or droplet size of dispersed phase and maximize the numbers of bubbles or droplets to obtain maximum mass transfer. Although, column, mixer-settler and other traditional contactors have been the workhorses of chemical industry for decades [1-2], but the limitations here is the interdependence of the two phases being contacted, which leads to difficulties such as separate extraction and stripping steps, requirement of multi-stage contactor for dilute streams, problems of emulsification, foaming, unloading, the need of density difference between the phases,

\* Corresponding to: Anil Kumar Pabby & M. L. Singh (email: dranilpabby@gmail.com & mlsingh@barc.gov.in)

DOI: <https://doi.org/10.11113/amst.v25n3.225>

requirement of large inventory etc [3, 4]; while the ion-exchange process encounters problems like resin fouling, capacity limitations, requirement of more complexing material and selectivity [5-6]. When the concentration level of the metal ion falls below the trace or ultra-trace levels, solvent extraction by using conventional contactors has its inherent limitation for the substantial uptake of metal ions owing to equilibrium limitation. Hence, it was prerequisite to develop a technique which overpower the above mentioned shortcomings. To meet this criteria, liquid membrane systems (LMs) have proved to be the promising candidates due to its high selectivity, low solvent and energy consumption, and simultaneous extraction and stripping etc [7-10]. Supported liquid membrane (SLM) is one of the LMs configurations, which comprises of microporous membrane having two membrane fluid phases interfaces immobilizes at two ends of the membrane pore. Liquid layer between the immobilized interfaces acts as a selective barrier which is responsible for solute transport. This technique has its own limitations due to low inventory of the membrane phase (in case planned for large concentration of solute), and issues related to membrane instability [7, 9, 11-15].

Dispersion liquid membrane (DLM) is another configuration of LMs, where one of the interface is mobile and the other interface is immobilized at membrane pore mouth. This configuration provides larger interfacial area for stripping compared to SLM technique and results higher mass transfer of solute from feed solution to recovery phase (Strippant). DLM is considered as stable membrane system due to constant supply of solvent to the membrane pores. That replenish liquid in the

membrane pore and solves the problem of solvent loss [16-20]. Due to short residence times of the dispersion in the contactor, DLM does not require the use of surfactant to stabilize the dispersion. This eases the product recovery process. The dispersion of strip phase in the organic phase is created externally in a mixer device. Multiple modules can be employed in series with countercurrent flow of the organic and aqueous phases based on the required extent of removal of the solute. Maintaining the quality of dispersion is important for avoiding interstage dispersification and pumping. A fine adjustment of the flow rate and cross membrane pressure is needed to avoid reduction in efficiency due to phase mixing across the pores [17].

Both the configurations can be operated in the hollow fiber membrane contactor. This is a shell and tube type contactor, where micro-porous lumens are in-housed in a shell. One fluid passes through the lumens and the other one in the shell side. Pseudo-emulsion based hollow fiber strip dispersion (PEHFSD) is a DLM technique, where a pseudo emulsion is formed by agitation of the two phases (strip dispersed in organic). Figure 1 shows a typical representation of the PEHFSD technique. This technique not only overcomes the stability problems associated with SLM but also adopts the merits of ELM with less energy being consumed. Here, a dispersion of strippant in organic phase (extractant and modifier) is passed through the shell side of the hollow fiber contactor, while feed solution containing metal ion is passed through the lumen side. Aqueous-organic phase interface is maintained at the pore mouth on the inner surface of the fiber by keeping the lumen side pressure slightly higher than that of the shell side. Microporous hollow fiber membrane modules provide an inexpensive, low

maintenance and dispersion free approach to continuous flow liquid-liquid extraction processes [21-27].

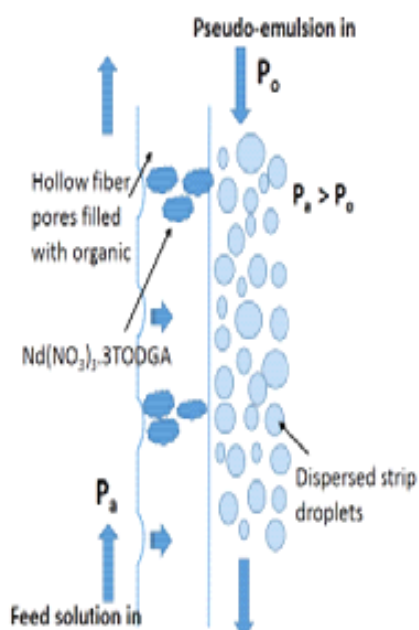


**Figure 1** A typical representation of PEHFS technique

The objective of the selection of Nd in present study is that neodymium is a surrogate of Am ( $\text{Am}^{241}$ : gamma energy-59 KeV and alpha energy 5.5 MeV). Of about 10-20 mg/l of americium (having a half-life of 435 years for  $\text{Am}^{241}$ ) from high level nuclear waste where  $\text{Am}^{241}$  is present as one of the minor actinide. This can be effectively separated from such solution using the present technique. The detailed study of the present work will help in studies on TODGA based americium separation. Some of the important previous work on Nd are described in Refs [28-30].

In order to accomplish systematic approach, performance evaluation based study and mathematical modelling of mass transfer of Nd in hollow fiber liquid membrane contactors was attempted. The parametric conditions studied include

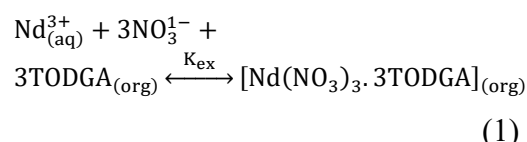
effect of aqueous to organic ratio (A/O) in dispersion, effect of speed of impeller on drop size formation, effect of feed acidity, effect of carrier concentration, effect of feed flow rate. Modelling not only helps in understanding the phenomenon better, but also helps in scaling up and optimization in design and operational parameters [17, 31-39]. Modelling for mass transfer processes incorporates the mathematical formulation of various steps involved in mass transport to predict the overall mass transfer flux followed by solving the formulated equations with the implementation of boundary conditions to obtain spatial and temporal variations of the concentration of the solute. Present work is an effort to study the extraction of neodymium (III) ( $\text{Nd}$ ) by using TODGA and  $\text{HNO}_3$  as the extractant cum stripping in PEHFS technique.

## 2.0 MODEL DEVELOPMENT

A model is developed to study the transport of Nd under different hydrodynamic and chemical conditions. A code is written to solve the model equations numerically to predict the feed reservoir concentration with time at different parametric conditions.

### 2.1 Chemistry

Extraction equilibrium for neodymium with TODGA can be expressed as:



Considering fast chemical reaction between the metal species and the membrane carrier, local equilibrium at interface is reached and concentrations at interface are related as below:

The Equilibrium extraction constant ( $K_{ex}$ ) is expressed as:

$$K_{ex} = \frac{[Nd(NO_3)_3 \cdot 3TODGA]_{(org)}}{[Nd^{3+}]_{(aq)} [NO_3^-]_{(org)}^3 [TODGA]_{(org)}^3} \quad (2)$$

Distribution coefficient of neodymium at the feed-membrane interface can be expressed as:

$$K_d = K_{ex} [NO_3^-]_{(org)}^3 [TODGA]_{(org)}^3 \quad (3)$$

It can be observed from the Equation (3) that distribution coefficient depends on the third power of nitrate ion and also on the third power of the TODGA concentration [15-16, 37].

## 2.2 Model Equation

Following are the assumptions considered in the process modelling of the extraction system:

- The reaction between the metal ion and ligand at aqueous membrane interface is instantaneous.
- Diffusion of the metal-ligand complex through the pores of the membrane in to the bulk of the organic phase is the rate controlling step
- Isothermal operation
- The organic phase in membrane pores has negligible solubility in the aqueous phase

In addition, membrane properties like membrane thickness, porosity and tortuosity are also considered.

Taking into account a single lumen, mass balance without accumulation (Figure 2) over a differential length  $\Delta z$  and time  $\Delta t$  can be written as [40]:

$$QC_{Nd} \Big|_z \Delta t = QC_{Nd} \Big|_{z+\Delta z} \Delta t + J_{org} (2\pi r \varepsilon \Delta z) \Delta t \quad (4)$$

Where,  $Q$  is volumetric flow rate,  $C_{Nd}$  is the neodymium concentration in the feed solution flowing through the lumen,  $J_{org}$  is the neodymium flux through the membrane pores, and  $r$  and  $\varepsilon$  are the inner radius and porosity of the hollow fiber lumen.

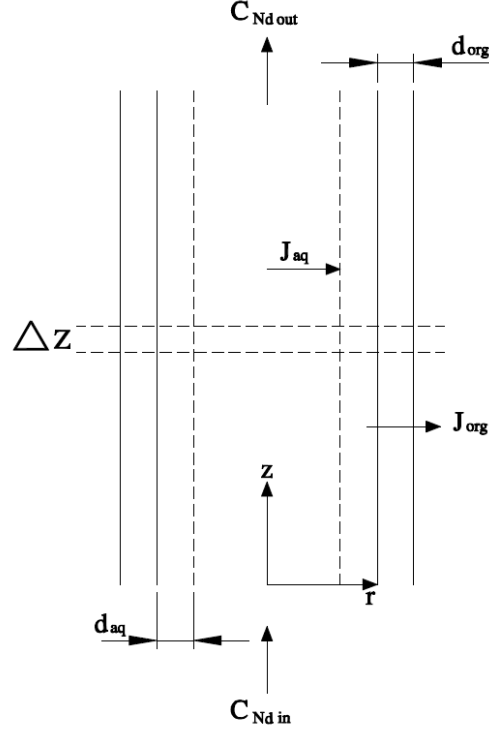


**Figure 2** Schematic representation of mass balance in a single lumen

Rearranging the Equation (4), we get:

$$J_{org} = -\frac{rv}{2\varepsilon} \frac{dC_{Nd}}{dz} \quad (5)$$

Where,  $v$  represents the linear flow velocity of aqueous feed in the lumen and  $z$  is the axial direction.

Mass transfer fluxes diffusing in the aqueous feed solution and passing through the membrane can be estimated by using Fick's first law of diffusion as:

$$J_{aq} = \frac{D_{aq} (C_{Nd} - C_i)}{d_{aq}} \quad (6)$$

$$J_{org} = D_{org} \frac{(\bar{C}_i - \bar{C}_i')}{\tau d_{org}} \quad (7)$$

Where,  $D$  is diffusion coefficient,  $\tau$  is the tortuosity and  $d_{aq}$  and  $d_{org}$  are the aqueous film thickness and membrane thickness, respectively. Diffusion coefficient can be calculated from Wilke and Chang correlation written in the Equation (8).

$$D = \frac{7.4 \times 10^{-8} (xM^{0.5}) \Gamma}{\eta (V_m^{0.6})} \quad (8)$$

Where,  $x$  is association factor,  $M$  is molecular weight of the solvent,  $T$  is temperature in kelvin,  $\eta$  is viscosity in centipoise and  $V_m$  is molar volume of the solute in cc/g.mol.

Thickness of aqueous layer can be estimated from the Leveque relation [18, 41-43] given below:

$$\frac{r}{d_{aq}} = 1.62 \left\{ \frac{d^2 v}{D_{aq}} \right\} \quad (9)$$

Considering distribution coefficient at the feed-membrane interface is much higher compared to the strip-membrane interface, Equation (7) can be written as:

$$J_{org} = \frac{D_{org} \bar{C}_i}{\tau d_{aq}} \quad (10)$$

Rate of mass transfer through the boundary layer will be equal to the rate of mass transfer through the membrane at any axial position and also equal to the overall mass transfer flux of the system under steady state condition i.e.

$$J_{aq} [2\pi l (r - d_{aq})] = J_{aq} 2\pi l r \epsilon \quad (11)$$

$$J_{aq} = J_{aq} \frac{r \epsilon}{(r - d_{aq})} \quad (12)$$

Combining Equation (5), Equation (6) and Equation (10) with Equation (12), we get:

$$\frac{dC_{Nd}}{dz} = - \frac{2\epsilon}{rv} \frac{K_d C_{Nd}}{\Delta_{aq} K_d + \Delta_{org}} \quad (13)$$

Where,  $\Delta_{aq}$  and  $\Delta_{org}$  are the resistances of the aqueous side and organic side, respectively and can be expressed as:

$$\Delta_{aq} = \frac{r \epsilon d_{aq}}{(r - d_{aq}) D_{aq}} \quad (14)$$

$$\Delta_{org} = \frac{d_{org} \tau}{D_{org}} \quad (15)$$

Integrating the Equation (13) over the effective hollow fiber length  $l$ , we get:

$$\int_{C_{Ndin}}^{C_{Ndout}} \frac{dC_{Nd}}{C_{Nd}} = - \frac{2\epsilon}{rv} \frac{K_d C_{Nd}}{\Delta_{aq} K_d + \Delta_{org}} \int_0^l dz \quad (16)$$

$$C_{Ndout} = C_{Ndin} e^{\left\{ \frac{2\epsilon}{rv} \left( \frac{K_d l}{\Delta_{aq} K_d + \Delta_{org}} \right) \right\}} \quad (17)$$

Balancing mass over the reservoir, we obtain:

$$\frac{dC_{Nd}}{dt} = - \frac{Q_f}{V_f} (C_{Ndout} - C_{Ndin}) \quad (18)$$

Where,  $Q_f$  and  $V_f$  are the feed flow rate and volume of the feed solution taken in the reservoir, respectively.

Rearranging Equation (17) and Equation (18) and integrating the equation with time interval  $t$ , we get the equation as:

$$\int_{C_{Nd0}}^{C_{Ndt}} \frac{dC_{Nd}}{C_{Nd}} = \int_0^t \frac{Q_f}{V_f} \left[ e^{\left\{ \frac{2\epsilon}{rv} \left( \frac{K_d l}{\Delta_{aq} K_d + \Delta_{org}} \right) \right\}} - 1 \right] dt \quad (19)$$

Integrating Equation (19), we obtain the result as:

$$\ln\left(\frac{C_{Nd_t}}{C_{Nd_0}}\right) = \frac{Q_f}{V_f} \left[ e^{\left\{ \frac{2\varepsilon}{rv} \left( \frac{K_d I}{\Delta_{aq} K_d + \Delta_{org}} \right) \right\}} - 1 \right] t \quad (20)$$

Where,  $C_{Nd_0}$  and  $C_{Nd_t}$  are the initial and final concentration of neodymium at  $t = 0$  and  $t = t$ , respectively.

### 2.3 Evaluation of Drop Size

Interfacial area always plays a key role on mass transfer and thus drop size in DLM processes. For a constant volume DLM system, higher emulsion drop size create less number of drops as compared to emulsions of small size and reduces the interface area for mass transfer. Fine drops increase interfacial area for stripping in PEHFSD processes and results higher recovery but makes process more energy intensive. Drop size forms in this process can be estimated by the empirical correlation written in the Equation (21).

$$\frac{a}{I_d} = 0.058(1 + 5.4\Phi)(We)^{-0.6} \quad (21)$$

Where,  $a$  is sauter mean diameter,  $I_d$  is impeller diameter,  $\Phi$  is volume fraction of the dispersed phase and  $We$  is the weber number. Weber number can be evaluated from the correlation written below.

$$We = \frac{\rho_c N^2 I_d^3}{\sigma} \quad (22)$$

Where,  $\rho_c$  is density of the continuous phase,  $N$  is speed of the impeller, and  $\sigma$  is surface tension of the dispersed phase.

### 3.0 EXPERIMENTS, MATERIALS AND METHODOLOGY

Experiments are conducted to evaluate mass transfer of neodymium at different hydrodynamic and chemical conditions. Figure 3 shows schematic representation of the extraction of Nd using PEHFSD technique. Details of the hollow fiber used is given in the Table 1. In this technique, pseudo emulsions are prepared by dispersing strip (0.001M  $HNO_3$ ) in the organic phase and passed through the shell side. Organic phase comprises of TODGA, *n*-dodecane and Isodecanol with composition (V/V) of 12.2 %, 65.1% and 22.7%, respectively. Emulsions are prepared at different aqueous to organic ratio ( $A/O = 1-6$ ) and at different speed of the agitator (490 rpm~ 1180 rpm). Feed solutions are prepared by dissolving Nd with different strength of nitric acid (1M-4M  $HNO_3$ ). Experiments are conducted at different parametric conditions to obtain the best extraction conditions. Collected raffinate samples are analyzed by inductively coupled plasma-atomic emission spectroscopy technique (ICP-AES technique). All the measurements are done at least in duplicate at room temperature and the obtained values are within  $\pm 2\%$  with good material balance ( $>98\%$ ).

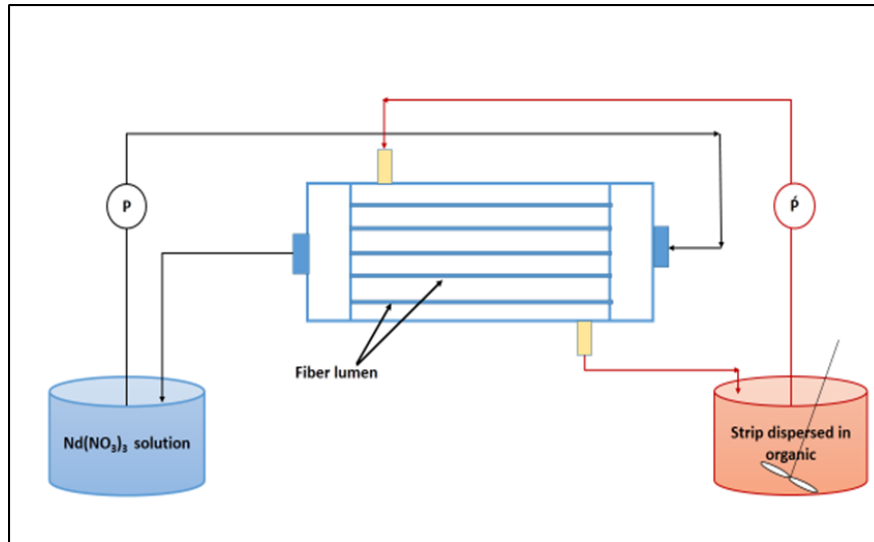


**Figure 3** Schematic representation of experimental set up

**Table 1** Details of the hollow fiber contactor

Parameters	Values
MOC of Lumen	Polypropylene
Module Diameter	8 cm
Module length	28 cm
Effective fiber length	15 cm
Internal Diameter of lumen	0.024 cm
Wall thickness of lumen	0.006 cm
Number of fibers	10000
Porosity of fibers	30%
Total membrane surface area	1.4 m <sup>2</sup>
Tortuosity of hollow fiber	3

## 4.0 RESULTS AND DISCUSSION

### 4.1 Transport of Nd at Different System Parameters

Transport of Nd is studied experimentally at different system parameters to obtain the optimum parametric conditions for the optimum output. Mass transfer of Nd is evaluated based on the feed reservoir concentration. Percentage extraction on Nd is estimated by the Equation (21).

$$\%E = \frac{(C_{Nd0} - C_{Ndt})}{C_{Nd0}} \cdot 100 \quad (21)$$

#### 4.1.1 Effect of Aqueous to Organic Ratio (A/O) in Dispersion on Nd Extraction

Figure 4 shows the effect of aqueous to organic ratio (A/O) in dispersion on percentage extraction of Nd. It can be seen from the figure that percentage extraction increases with increase in A/O ratio of dispersion from 1 to 4. By increasing A/O ratio, diffusion length of the membrane phase gets reduced which in turn increases availability of more mass transfer area of strippant per unit volume of organic. This enhancement on percentage is due to fast recovery of Nd from the organic phase by diffusion and stripping. This is due to more TODGA being available

for a fixed volume of feed. As A/O ratio increases further to 6, the percentage extraction of  $N_d$  decreases which may be due to the less volume of the extractant available for extraction. In addition, instability of

the pseudo-emulsion formed with insufficient amount of TODGA can affect the transport of  $N_d$ . Hence, A/O=4 is fixed for all the studies under similar experimental conditions.

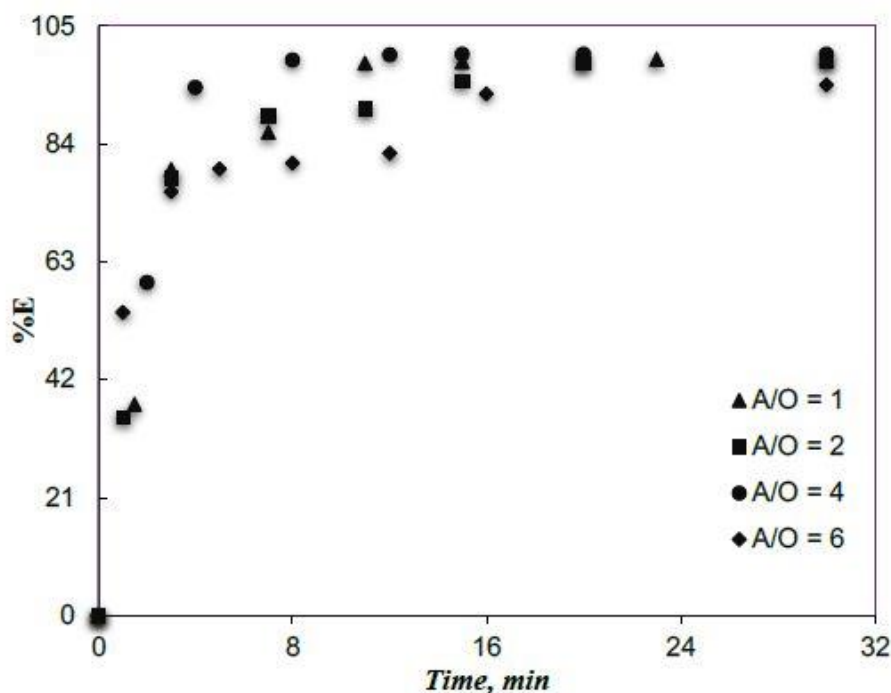


**Figure 4** Effect of A/O ratio in dispersion on extraction of  $N_d$

#### 4.1.2 Effect of Speed of Impeller on Drop Size Formation and Percentage Extraction of $N_d$

Speed of the agitator plays a key role on the size of pseudo-emulsion. Drop size is estimated by using the correlation mentioned in the Equation (21). Figure 5 shows the effect of speed of the agitator on the souter mean diameter of the emulsion. It can be evident from the figure that drop diameter decreases with increase in speed of the impeller. This is due to the more input of energy with higher RPM. Effect of drop size on percentage extraction of  $N_d$  is shown in the Figure 6. Percentage of extraction increases with reduction in drop size from 1.22 mm to 0.41mm due to decrease in the

diffusion length on the membrane phase. Formation of bigger drop size reduces the total number of emulsion globules formed at low RPM as compared to smaller drop size formed at higher RPM in the same volume system. Thus total mass transfer area available is less for bigger emulsion drops as compared to the smaller size emulsion droplets. With further reduction of drop size into 0.22 mm reduces percentage extraction. This can be attributed to the increase in resistance owing to the rigid nature of the droplets where no internal circulation occurs. Speed of the impeller is maintained 980 RPM for all the further studies where the emulsion drop size is of 0.41 mm.

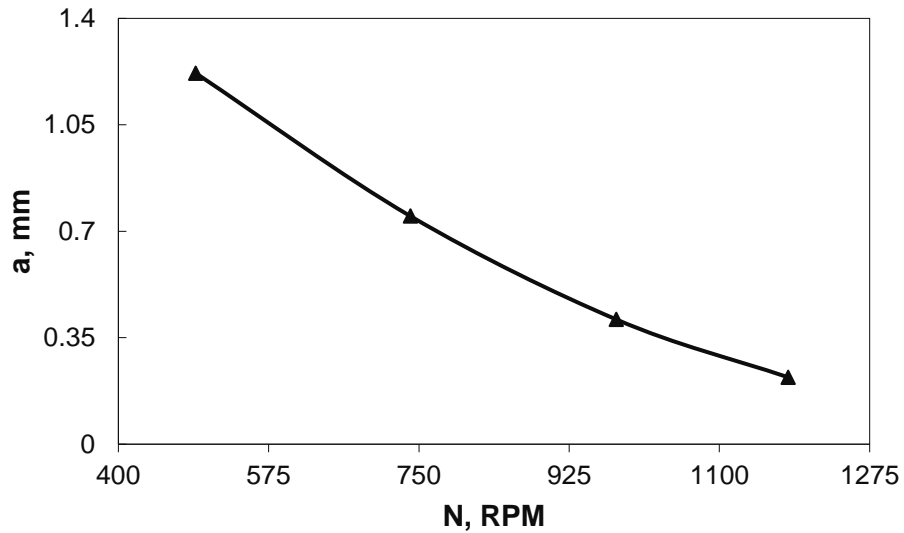


**Figure 5** Effect of speed of impeller on formation of emulsion drop size

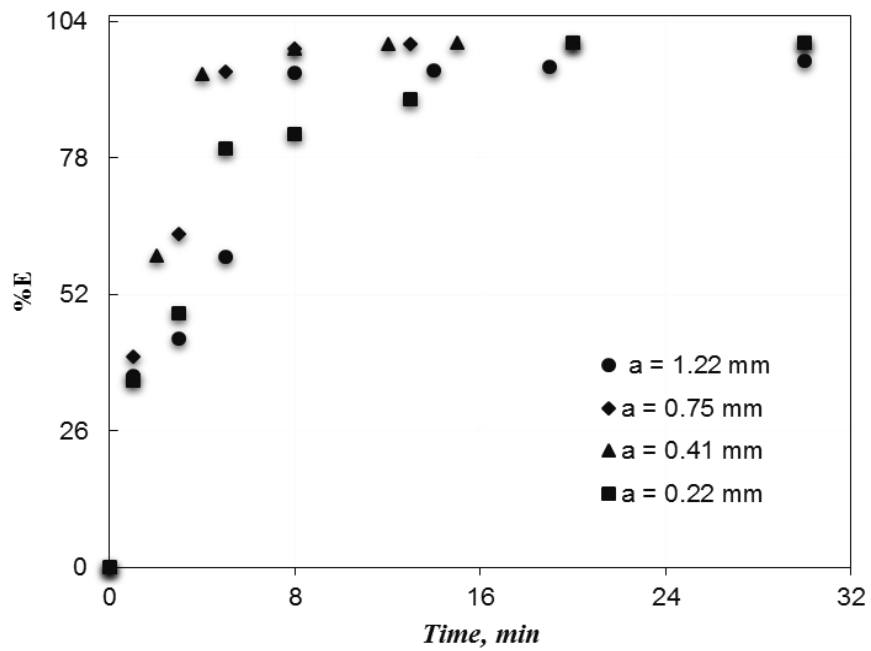


**Figure 6** Effect of emulsion droplet size on percentage extraction of  $N_d$ ; ( $N_{d0} = 1 \text{ g/L}$ ,  $(H_f)^+ = 3.5 \text{ M}$ ,  $A/O = 4$ , Agitator speed = 980 RPM)

**4.1.3 Effect of Feed Acidity on Percentage Extraction  $N_d$**

Effect of feed acidity on percentage extraction of  $N_d$  is shown in the Figure 7. Rate of transport of  $N_d$  increases with increase in feed acidity. This can

be attributed to the co-transportation of  $NO_3$  ion along with  $N_d$  Equation (1). This enhance driving force for  $N_d$  transport. Feed acidity is maintained 3.5 M for all the extraction study of the  $N_d$ .

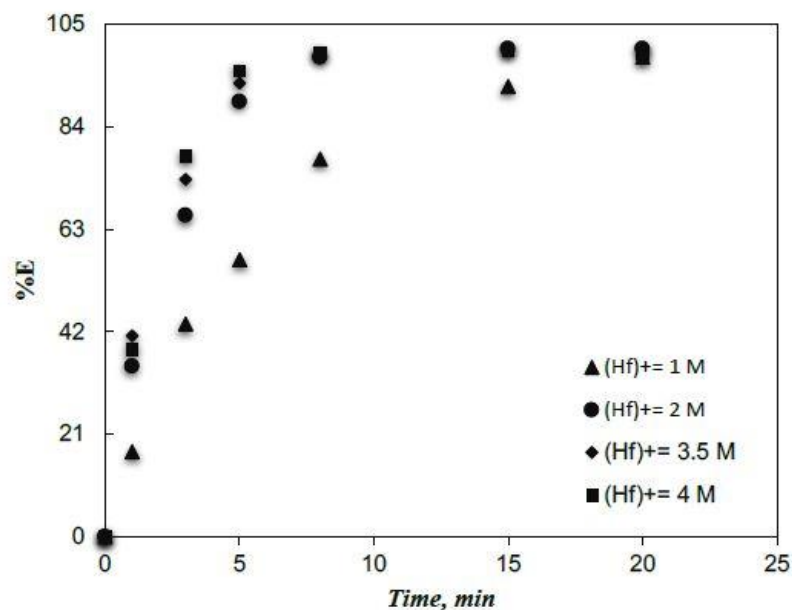


**Figure 7** Effect of feed acidity on percentage extraction of Nd; ( $N_{d0} = 1$  g/L,  $(H_f)^+ = 3.5$  M, A/O =4, Agitator speed = 980 RPM

## 4.2 Model Validation

Mass transfer is obtained by solving Equation (20) discussed in the section 2.3 by solving numerically. A code is written to solve the equation to obtain the raffinate concentration of Nd with time. Percentage of extraction is estimated by the Equation (21). Results of the simulation under different hydrodynamic and chemical parameters are validated with the experimental results.

### 4.2.1 Effect of Feed Acidity

Figure 8 shows the mass transfer of neodymium at different feed acidity. It can be observed from the graph that percentage extraction of neodymium increases with increase in feed acidity. Mass transfer of neodymium reaches close to 90 % as feed acidity increases from 1 M to 3.5 M. This can be attributed to increase in distribution coefficient due to increase in feed acidity. The same can be observed in

the Equation (3) also that distribution coefficient values are influenced by the 3<sup>rd</sup> power of  $[\text{NO}_3^-]$  ion concentration. This gives a driving force for neodymium transfer. Simulated results are validated with experimental results and was found in good agreement. With further increase in feed acidity to 4 M, rise in extraction of neodymium is insignificant. There may be increase in  $[\text{NO}_3^-]$ -TODGA complexation and results in decrease in the neodymium transport.

### 4.2.2 Effect of Carrier Concentration

Effect of carrier concentration on mass transfer of neodymium is shown in the Figure 9. It can be evident from the figure that percentage extraction of neodymium with time increases with increase in concentration of TODGA from 0.1 M to 0.5 M, which is because of increase in distribution coefficient. Increase in TODGA concentration enhances complexation of Nd-TODGA

at the feed membrane interface and results higher mass transfer of neodymium. It can be evident from the Equation (3) that distribution coefficient is influenced by the 3<sup>rd</sup> power of TODGA concentration. The transport rate was therefore limited by

diffusion through the aqueous film on the feed side of membrane in this region. Simulated results are validated with the experimental results and found in agreement with experimental data.

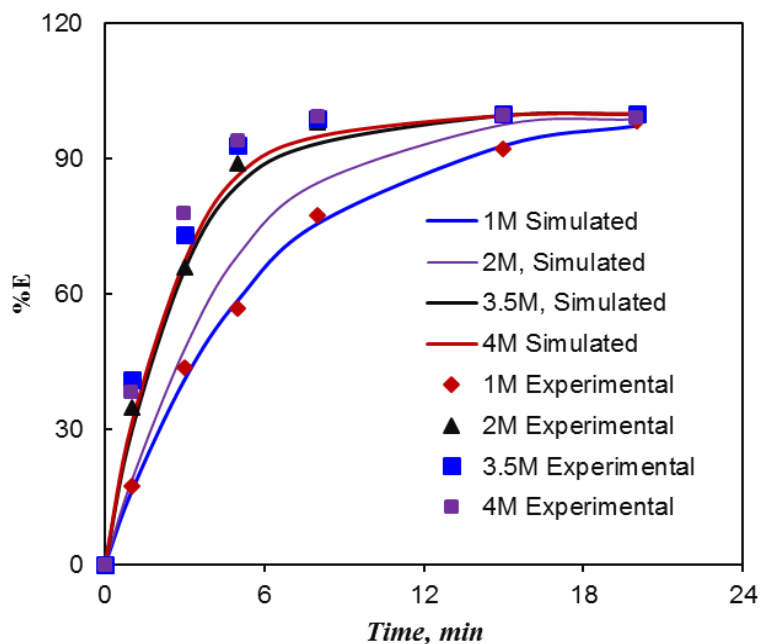


**Figure 8** Effect of feed acidity on neodymium transfer ( $Nd_0 = 1 \text{ g/L}$ ,  $(H_f) = 3.5 \text{ M}$ , TODGA concentration =  $0.2 \text{ M}$ , A:O = 1:4, speed of agitator = 980 rpm)

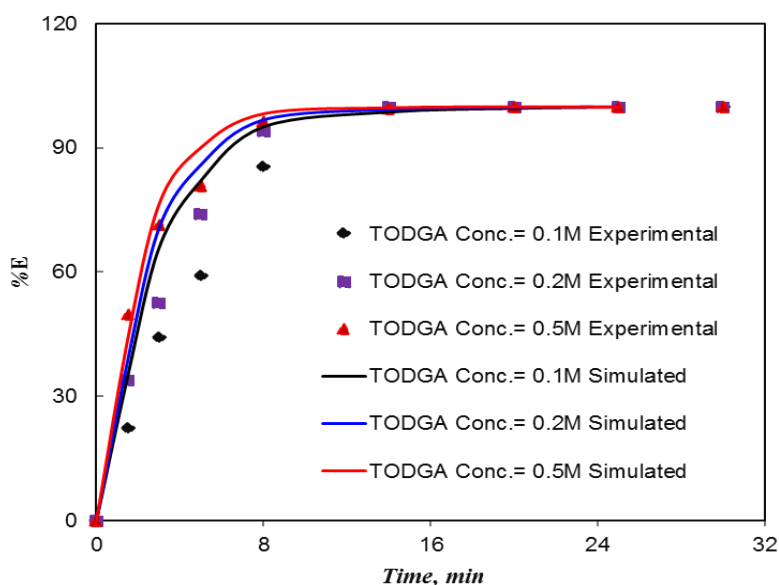


**Figure 9** Effect of TODGA concentration on neodymium transfer ( $Nd_0 = 2 \text{ g/L}$ ,  $(H_f) = 3.5 \text{ M}$ , A/O = 4, speed=980 rpm)

### 4.2.3 Effect of Feed Concentration

Figure 10 shows the percentage extraction of Nd plotting initial feed concentration against time. It can be seen from the figure that percentage extraction of Nd decreases with increase in the initial feed concentration. This can be attributed to the more inlet flux enters with higher initial concentration into the hollow fiber contactor and also the equilibrium

limitations dominated the mass transfer process. Therefore, the Nd transport rate is determined by the rate of diffusion of Nd-containing species through the feed diffusion layer and the rate of Nd-TODGA species through the membrane. This can be further enhanced by increasing carrier concentration. Several studies have observed similar behavior by increasing the inlet concentration.

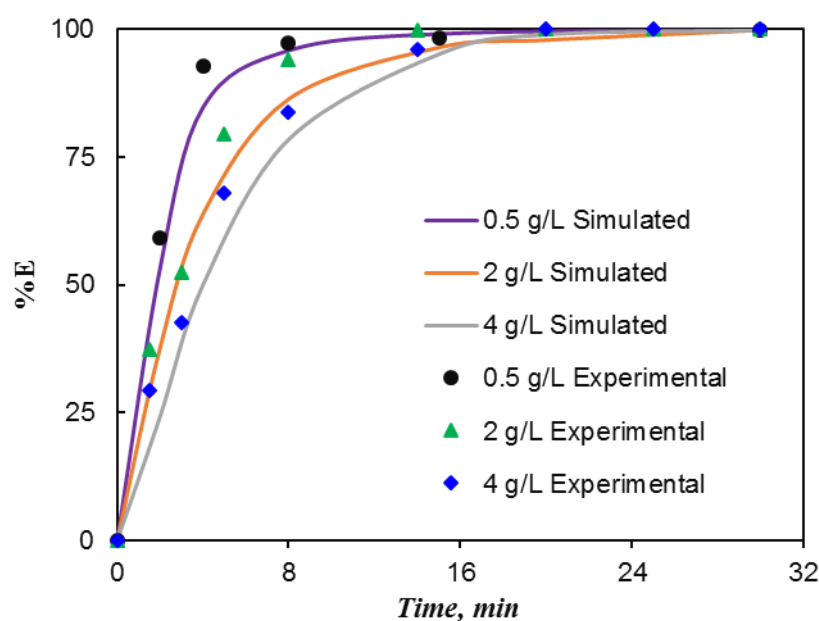


**Figure 10** Effect of initial feed concentration on extraction of Nd ( $Nd_0 = 2\text{g/L}$ ,  $(H_f) = 3.5\text{ M}$ ,  $A/O = 4$ , speed=980 rpm)

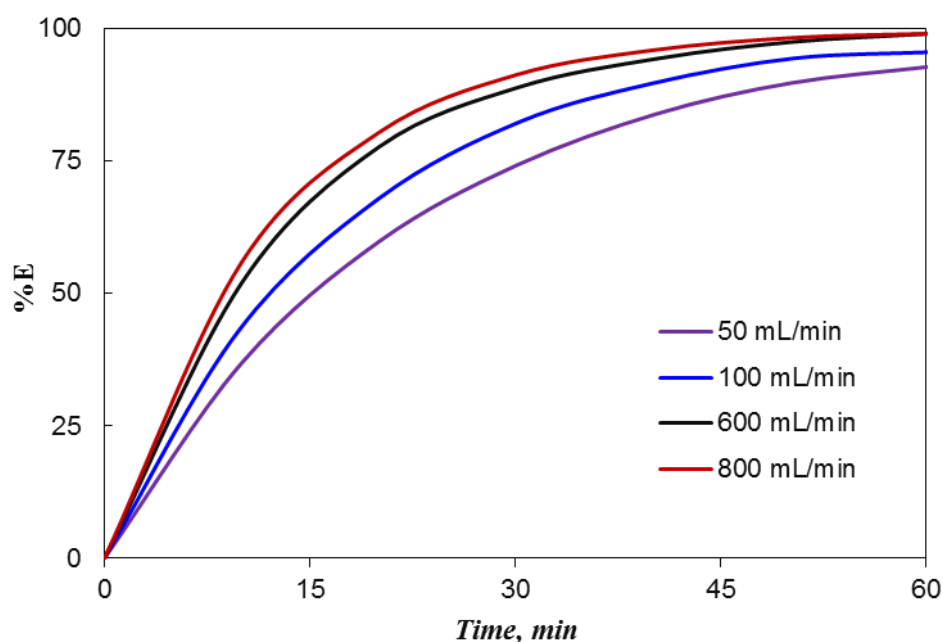
### 4.2.4 Effect of Feed Flow Rate

Figure 11 shows the effect of feed velocity on percentage extraction of Nd obtained from the simulation. Percentage extraction increases with increase in feed flow rate. Slope of the curve increases significantly from 50 mL/min to 100 mL/min and to 600 mL/min. The increase of Nd transport with linear flow rate was caused by a decrease in the thickness of the aqueous boundary layer ( $\Delta_{aq}$ ) at the inner radius of lumen) when the linear

feed flow rate in the fiber lumen increased. This finally resulted in reduction of resistances on the feed side which in turn enhances mass transfer coefficient and thus increase in the percentage extraction. Further rise in the feed velocity to 800 mL/min does not influence percentage extraction significantly. This may be due to the very less reduction of feed resistance further to 600 mL/min. The other reason for a decrease in % transport of Nd could be lower residence time at higher flow rates,

which provides insufficient time to complex Nd with TODGA. This resulted in incomplete loading of

TODGA with Nd, which finally contributed to the lower % of Nd.



**Figure 11** Effect of feed flow rate on percentage extraction of  $N_d$  ( $N_{d0} = 1$  g/L,  $(H_f)^+ = 3.5$  M,  $Q_e = 500$  mL/min)

## 5.0 CONCLUSIONS FUTURE PERSPECTIVE

PEHFSD technique is a novel technique for the recovery of  $N_d$  from dilute streams. This method seems to be a promising alternative process due to its stability, simplicity and cost of operation. This is an efficient process due to its high surface area for extraction as well as stripping, and low energy consumption for creating the pseudo-emulsion and for the separation of phases. This technique takes the combine advantages of emulsion liquid membrane and overcomes the sufferings of supported liquid membrane due to membrane stability. Extraction of  $N_d$  is studied in a hollow fiber contactor, with strip (0.01 M nitric acid) dispersed in organic mixture of TODGA, isodecanol and *n*-dodecane (0.2 M TODGA) able to recover 99.7%  $N_d$  from the feed streams on recycle mode of operation.

This technique needs low inventory of organic as compared to non-dispersive solvent extraction technique. Mathematical model is developed to study the extraction of  $N_d$  and a code is written to solve the transport equations with appropriate initial conditions. Mass transfer resistances and diffusivity have been estimated by the empirical correlations. The  $K_d$  value was determined to be 699.1 (at 0.2 M TODGA, 3.5 M  $HNO_3$ ) and order of diffusivities i.e.  $D_{org}$  and  $D_{aq}$  were  $10^{-7}$  and  $10^{-6}$   $cm^2/s$  respectively. Experiments are conducted at different parametric conditions to obtain the optimum extraction conditions. Results obtained from the simulation is validated with the experimental data. Present study will not only help to understand the  $N_d$  extraction process with its design and scale-up but also help to TODGA based americium separation in the back end of nuclear fuel cycle.

## REFERENCES

- [1] A. K. Pabby, S. R. Wickramasinghe, K. K. Sirkar, A. M. Sastre. 2020. *Hollow Fiber Membrane Contactors: Module Fabrication, Design and Operation, and Potential Applications*. CRC Press: Boca Raton, FL, USA.
- [2] A. K. Pabby, S. S. H. Rizvi, A. M. Sastre. 2008. *Handbook of Membrane Separations: Chemical, Pharmaceutical, Food, and Biotechnological Applications*. 2<sup>nd</sup>. CRC Press: Boca Raton, FL, USA.
- [3] M. Cox, S. Alegert, Ed. 1998. *Developments in Solvent Extraction*. Ellis Horwood; Chichester. 177.
- [4] P. R. Danesi, In: S. Alegert, Ed. 1998. *Developments in Solvent Extraction*. Ellis Horwood; Chichester. 159.
- [5] X. J. Yang, A. G. Fane and K. Soldenhoff. 2003. Comparison of Liquid Membrane Processes for Metal Separations: Permeability, Stability and Selectivity. *Ind. Eng. Chem. Res.* 42: 392-403.
- [6] S. E. Kentish and G. W. Stevens. 2001. Innovations in Separation Technology for Recycle and Reuse of Liquid Waste Streams. *Chemical Engng. J.* 84: 149-159.
- [7] J. Song. 2018. A Critical Review on Membrane Extraction with Improved Stability: Potential Application for Recycling Metals from City Mine. *Desalination*. 440: 18-38. DOI: 10.1016/j.desal.2018.01.007.
- [8] P. K. Parhi., S. S. Behera., R. K. Mohapatra, T. R. Sahoo, D. Das, P. K. Misra. 2019. Separation and Recovery of Sc(III) from Mg–Sc Alloy Scrap Solution through Hollow Fiber Supported Liquid Membrane (HFLM) Process Supported by Bi-functional Ionic Liquid As Carrier. *Separation Science and Technology*. 54: 1478-1488.
- [9] A. M. Sastre, A. K. Pabby, J. P. Shukla, R. K. Singh. 1998. Improved Techniques in Liquid Membrane Separation: An Overview. *Sep. Purif. Methods*. 27: 213.
- [10] A. K. Pabby, A. M. Sastre. 2013. State-of-the-art Review on Hollow Fiber Contactor Technology and Membrane-Based Extraction Processes. *J. Membr. Sci.* 430: 263-303.
- [11] N. M. Kochrginsky, Q. Yang and L. Seelam. 2007. Recent Advances in Supported Liquid Membrane Technology. *Separation Purification Technology*. 53: 171-177.
- [12] C. Hill, F. Dozol, H. Rouquette, S. Eymard and B. Tournois. 1996. Study of Stability of Some Supported Liquid membranes, *Journal of Membrane Science*. 114: 73-80,
- [13] A. K. Pabby, Swain, B., Sastre, A. M. 2017. Recent Advances in Smart Integrated Membrane Assisted Liquid Extraction Technology, *Chemical Engineering and Processing: Process Intensification*. *Chem. Eng. Process.* 120: 27-56. DOI: 10.1016/j.cep.2017.06.006.
- [14] F. F. Jha, A. G. Fane, and C. J. D. Fell. 1995. Effect of Surface Tension Gradients on the Stability of Supported Liquid Membranes. *Journal of membrane Science*. 107: 75-86.
- [15] P. R. Dansi, L. Reichley-Yinger and P. G. Rickert. 1987. Life Time of Supported Liquid Membranes, the Influence of Interfacial Properties, Chemical Composition, and Water Transport on the Long Term

- Stability of the Membranes  
*Journal of Membrane Science*.  
31: 117-145.
- [16] A. K. Pabby, S. R. Wickramasinghe, K. K. Sirkar, and A. M. Sastre. 2020. Process Intensification in Integrated Use of Hollow Fiber Contactor-based Processes: Case Studies of Sparkling Water Production and Membrane Contactor-Based Strip Dispersion Proces. *Hollow Fiber Membrane Contactors: Module Fabrication, Design and Operation, and Potential Applications*, Pabby, Wickramasinghe, Sirkar, Sastre (Eds.). CRC Press. Chap. 8, FL, USA.
- [17] S. Mukhopadhyay, S. Mishra, K. T. Shenoy, V. A. Juvekar. 2020. Application of Hollow Fiber Contactor for Polishing of Lean, Streams Containing Uranium from Nuclear Industry: Scale up and Demonstration. *Hollow Fiber Membrane Contactors: Module Fabrication, Design and Operation, and Potential Applications*, Pabby, Wickramasinghe, Sirkar, Sastre (Eds.). CRC Press. Chap. 9, FL, USA.
- [18] A. Gabelman, S. Hwang. 1999. Hollow Fiber Membrane Contactors. *J. Membr. Sci.* 159: 61.
- [19] A. K. Pabby, J. V. Sonawane, A. M. Sastre, Y. Kulkarni. 2015. Industrial Applications of Membrane Contactors. A. K. Pabby, S. S. H. Rizvi, A. M. Sastre. (Eds.). *Hand Book of Membrane Separations: Chemical, Pharmaceutical Food and Biotechnological Application*. Second Edition. CRC Press, Boca Raton, FL. 53-76, Chapter 4.
- [20] W. Rongwong, K. Goh. 2020. Resource Recovery from Industrial Wastewaters by Hydrophobic Membrane Contactors: A Review. *Journal of Environmental Chemical Engineering*. 8: 104242.
- [21] J. V. Sonawane, A. K. Pabby, A. M. Sastre. 2008. Pseudo Emulsion based Hollow Fiber Strip Disoersion (PEHFSD) Technique: Novel Methodology for Gold Recovery from Base Metals in Cyanide Media. *AIChEJ.* 54: 453-463.
- [22] A. Wojciechowska, M. T. A. Reis, I. Wojciechowska, M. R. C. Ismael, M. L. F. Gameiro, K. Wieszczycka, J. M. Carvalho. 2018. Application of Pseudo-Emulsionbased Hollow Fiber Strip Dispersion with Task-Specific Ionicliquids for Recovery of Zinc(II) from Chloride Solutions. *Journal of Molecular Liquids*. 254: 369-376.
- [23] I. Garcia-Diaz, F. A., Lopez, F. J. Alguacil, Transportof Indium(III) using Pseudo-emulsion based Hollow Fiberstrip Dispersion with Ionic Liquid  $\text{RNH}_3+\text{HSO}_4^-$ . *Chemical Engineering Research and Design*. 126: 134-141.
- [24] K. Staszak A. Wojciechowska, M. T. A. Reis, I., Wojciechowska, K. Wieszczycka, M. R. C., Ismael, J. M. R., Carvalho. 2017. Recovery of Zinc(II) from Chloride Solutions using Pseudo-emulsion based Hollow Fiber Stripdispersion with Pyridineketoxime Extractants. *Separation and Purification Technology*. 177: 152-160.
- [25] M. Fourie, D. J. van der Westhuizen, H. M. Krieg. 2018. Uranium Recovery and Purification from Simulated Waste Streams Containing High

- Uranium Concentrations with Dispersion Liquid Membranes. *Journal of Radio Analytical and Nuclear Chemistry*. 317: 355-366.
- [26] Himanshu, P. Kohli, Smita Gupta, Mousumi Chakraborty. 2020. Characterization and Stability Study of Pseudo-Emulsion Hollow Fiber Membrane: Separation of Ethylparaben. *Colloids and Surfaces A*. 587: 124308.
- [27] M. T. A. Reis, M. R.C. Ismael, A. Wojciechowska, I., Wojciechowska, P. Aksamitowski, K. Wieszczycka, J. M. R., Carvalho. Zinc(II) Recovery using Pyridineoxime-ether – Novel Carrier in Pseudo-Emulsion Hollow Fiber Strip Dispersion System. *Separation and Purification Technology*. 223: 168-177.
- [28] Y. D. Jagdale, P. V. Vernekar, A. W. Patwardhan, A. V. Patwardhan, S. A. Ansari, P. K. Mohapatra, and V. K. Manchanda. 2013. Mathematical Model for the Extraction of Metal Ions Using Hollow Fiber Supported Liquid Membrane Operated in a Recycle Mode. *J. Sep. Sci. Technol.* 48: 1-14.
- [29] T. Wannachod, N. Leepipatpiboon, U. Pancharoen, K. Nootong. 2014. Separation and Mass Transport of Nd (III) from Mixed Rare Earths via Hollow Fiber Supported Liquid Membrane: Experiment and Modelling. *Chem. Eng. J.* 248: 158-167.
- [30] T. Wannachod, N. Leepipatpiboon, U. Pancharoen, S. Phatanasri. 2015. Mass Transfer and Selective Separation of Neodymium Ions via a Hollow Fiber Supported Liquid Membrane using PC88A as Extractant. *J. Ind. Eng. Chem.* 21: 535-541.
- [31] B. E. San Roman, M. F., J. A. Irabien and A. Ortiz. 2009. An Over View of the Mathematical Modelling of Liquid Membrane Separation Processes in Hollow Fiber Contactors. *J. Chem. Technol. Biotechnol.* 84: 1583-1614.
- [32] B. Swain, and A. K. Pabby. 2015. Different Aspects of Mathematical Modeling in Hollow Fiber Liquid Membranes. *International Conference on Membrane based Separations (MEMSEP-2015), 21-23 March 2015, M S University, Vadodara, Gujarat, India.*
- [33] B. Swain, K. K. Singh, and A. K. Pabby. 2018. Mass Transfer Modelling in Hollow Fiber Liquid Membrane Separation Process. Sridhar Sundergopal, Kumar Saranya Ramesh, Membrane Technology Sustainable Solutions in Water, Health, Energy and Environmental Sectors. CRC Press, Boca Raton, FL. Chapter 12: 253-275.
- [34] Smita Dixit, S. Mukhopadhyay, Smita Govalkar, K. T. Shenoy, H. Rao and S. K. Ghosh. 2012. A Mathematical Model for Pertraction of Uranium in Hollow Fiber Contactor using TBP. *J. Desalination and Water Treatment*. 38: 195-206.
- [35] Ivan Červeňansky, Mario Mihaľ, Jozef Markoš. 2019. Pertraction-adsorption In Situ Product Removal System: Design and Mathematical Modelling. *Chemical Engineering & Processing: Process Intensification*. 143: 107604.
- [36] D. N. Ambre, S. A. Ansari, M. Anitha, P. Kandwal, D. K. Singh, H. Singh and P. K. Mohapatra. 2013. Non- Dispersive Solvent

- Extraction of Neodymium using a Hollow Fiber Contactor: Mass Transfer and Modelling Studies, *Journal of Membrane Science*. 446: 106-112.
- [37] P. V. Vernekar, A. W. Patwardhan, A. V. Patwardhan, S. A. Ansari, P. K. Mohapatra and V. K. Manchanda. 2013. Mathematical Modelling for the Extraction of Neodymium from Nitrate Media using Hollow Fiber Supported Liquid Membrane Operated in a Recycling Mode. *J. Separation Science and Technology*. 48: 1003-1014.
- [38] Arefeh Azarang, Ahmad Rahbar-Kelishami, Reza Norouzbeigi, Hadi Shayesteh. 2019. Modeling and Optimization of Pertraction Performance of Heavy Metal Ion from Aqueous Solutions using M2EHPA/D2EHPA: Application of Response Surface Methodology. *Environmental Technology & Innovation*. 15: 100432.
- [39] G. Pandey, M. Paramanik, S. Dixit, S. Mukhopadhyay, R. Singh, S. K. Ghosh, K. T. Shenoy. 2017. Extraction of Zirconium from Simulated Acidic Nitrate Waste Using Liquid Membrane in Hollow Fiber Contactor. *Desalination and Water Treatment*. 90: 63-69.
- [40] Smita Dixit, S. Mukhopadhyay, Smita Govalkar, K. T. Shenoy, H. Rao and S. K. Ghosh. 2012. A Mathematical Model for Pertraction of Uranium in Hollow Fiber Contactor using TBP. *J. Desalination and Water Treatment*. 38: 195-206.
- [41] P. Kandwal, S. Dixit, S. Mukhopadhyay and P. K. Mohapatra. 2011. Mass Transport Modelling of Cs(I) through Hollow Fiber Supported Liquid Membrane Containing calix-[4]-bis (2,3-naphtho)-crown-6 as the Mobile Carrier. *Chemical Engineering Journal*. 174: 110-116.
- [42] E. L. Cussler. 1988. *Diffusion-mass Transfer in Fluid Systems*. 1st Ed. Cambridge University Press, New York.
- [43] A. H. P. Skelland. 1974. *Diffusional Mass Transfer*. Wiley, New York.